genesis 50:700–710 (2012)

TECHNOLOGY REPORT

Generation and Characterization of a Notch1 Signaling-Specific Reporter Mouse Line

Emma Smith,[1] Stéphanie Claudinot,[2,3] Rajwinder Lehal,[1] Luca Pellegrinet,[1] Yann Barrandon,[2,3] and Freddy Radtke[1]*

[1]Swiss Institute for Experimental Cancer Research (ISREC), School of Life Sciences, Ecole Polytechnique Fédérale de Lausanne (EPFL), 1015 Lausanne, Switzerland

[2]Department of Experimental Surgery, Lausanne Medical School, CHUV, 1011 Lausanne, Switzerland

[3]Laboratory of Stem Cell Dynamics, School of Life Sciences, Ecole Polytechnique Fédérale de Lausanne (EPFL), 1015 Lausanne, Switzerland

Received 24 February 2012; Accepted 27 March 2012

Summary: Signaling through the Notch1 receptor is essential for the control of numerous developmental processes during embryonic life as well as in adult tissue homeostasis and disease. Since the outcome of Notch1 signaling is highly context-dependent, and its precise physiological and pathological role in many organs is unclear, it is of great interest to localize and identify the cells that receive active Notch1 signals in vivo. Here, we report the generation and characterization of a BAC-transgenic mouse line, N1-Gal4VP16, that when crossed to a Gal4-responsive reporter mouse line allowed the identification of cells undergoing active Notch1 signaling in vivo. Analysis of embryonic and adult N1-Gal4VP16 mice demonstrated that the activation pattern of the transgene coincides with previously observed activation patterns of the endogenous Notch1 receptor. Thus, this novel reporter mouse line provides a unique tool to specifically investigate the spatial and temporal aspects of Notch1 signaling in vivo. genesis 50:700–710, 2012. **© 2012 Wiley Periodicals, Inc.**

Key words: Notch1; signaling; reporter mouse line

The Notch cascade regulates many cellular differentiation events through cell-to-cell communication in a context- and dose-dependent manner during embryonic and postnatal development. In addition, dysfunctional Notch signaling results in a large variety of developmental defects as well as adult pathologies including cancer (reviewed in Artavanis-Tsakonas and Muskavitch, 2010). The *Notch* genes (*Notch1–Notch4* in mammals) encode single transmembrane cell surface receptors, which are bound by the Delta and Jagged family members of ligands on neighboring cells. Notch signaling is initiated by receptor–ligand interaction that elicits two consecutive proteolytic cleavages, S2 (Mumm *et al.*, 2000) and S3 (Schroeter *et al.*, 1998), mediated by the metalloproteases of the ADAM family (Brou *et al.*, 2000) and a γ-sectreatese complex (De Strooper *et al.*, 1999), respectively. The last cleavage liberates the intracellular domain of Notch (NIC), which translocates to the nucleus (Struhl and Adachi, 1998). Once in the nucleus, NIC associates with the DNA binding protein CSL/RBPJκ (Fortini and Artavanis-Tsakonas, 1994; Jarriault *et al.*, 1995) thereby recruiting other coactivators and initiates the formation of a functional transcription activation complex driving target gene expression (Kurooka and Honjo, 2000; Oswald *et al.*, 2001; Wallberg *et al.*, 2002; Wu *et al.*, 2000).

The role of Notch signaling is known to be highly context-dependent and the molecular factors that deter-

Current address for Emma Smith: Center for Molecular Pathology, Department of Laboratory Medicine, Lund University, University Hospital SUS, 20502 Malmö, Sweden.

*Correspondence to: Freddy Radtke, Ecole Polytechnique Fédérale de Lausanne (EPFL), Swiss Institute for Experimental Cancer Research (ISREC), Station 19, 1015 Lausanne, Switzerland.

E-mail: freddy.radtke@epfl.ch

Contract grant sponsors: Swiss National Scienc Foundation, the Marie Curie Foundation (NotchIT), EuroSyStem, OptiStem, Wenner-Gren Foundations.

Published online 7 April 2012 in Wiley Online Library (wileyonlinelibrary.com).

DOI: 10.1002/dvg.22030

mine the final outcome of Notch signaling in a particular cell type or tissue remain to be fully elucidated. This gap in knowledge is in part due to the inability to identify cell populations receiving an active Notch signal in vivo. Several reporter mice have been generated to address this issue (Basak and Taylor, 2007; Duncan *et al*., 2005; Fre *et al*., 2011; Imayoshi *et al*., 2010; Ohtsuka *et al*., 2006; Souilhol *et al*., 2006; Vooijs *et al*., 2007); however, all of them have certain limitations. Some strategies aim to visualize endogenous Notch receptor activity, in which reporter expression is driven by promoter regions of the Notch target genes *Hes1* or *Hes5* (Basak and Taylor, 2007; Fre *et al*., 2011; Imayoshi *et al*., 2010; Ohtsuka *et al*., 2006), or by multimerized RBPJκ-binding sites (Duncan *et al*., 2005; Souilhol *et al*., 2006). Nevertheless, Hes reporters can become activated by alternative signaling pathways and thus are not restricted to Notch-specific activation. The transgenic reporter mouse based on multimerized RBP-jκ binding sites is Notch specific, but it is unclear through which of the four receptors the signal is initiated. Notch receptor-specific reporter lines have indeed been generated either by replacing the cytoplasmic domain of Notch1 with a cDNA coding for the cre recombinase (Vooijs *et al*., 2007) or by knocking in a Cre-ERT2 gene into the ATG of the different Notch receptors (Fre *et al*., 2011). Although receptor specific, these systems do not discriminate between cells that receive an active Notch signal and cells descending from a Notch signaling precursor. The reporter systems based on expression of Cre-ERT2 from different Notch loci reflect Notch receptor expression but not necessarily signaling.

Here, we report the generation of an alternative reporter system designed to detect cells receiving an active Notch1 signal in vivo. The strategy is based on the generation of a chimeric Notch1 receptor, in which NIC is replaced by GAL4-VP16 (N1-Gal4VP16). The Notch1-specific proteolytic cleavage sites necessary for ligand-induced activation are preserved in this chimeric receptor (Fig. 1a). The functionality of the N1-Gal4VP16 protein was initially confirmed in a coculture assay (Fig. 1b), indicating that mechanistically the ligand-dependent activation of N1-Gal4VP16 is identical to endogenous Notch1 receptor activation.

As Notch1 signaling is dose dependent, we did not want to interfere with the endogenous Notch1 locus through gene targeting. Therefore, to ensure that the in vivo expression of N1-Gal4VP16 mirrored that of endogenous *Notch1*, we opted for a transgenic approach using a bacterial artificial chromosome (BAC) spanning a region 125 kb upstream and 30 kb downstream of the first and last coding exon of *Notch1*, respectively. We inserted the coding sequence for N1-Gal4VP16 into the BAC at the start codon present in the first coding exon of *Notch1* via homologous recombination (Fig. 1c) (Gong *et al*., 2002; Sparwasser *et al*., 2004). Correct targeting of the BAC was verified by PCR and Southern blot analysis (data not shown, and Fig. 1d). The modified BAC was injected into the pronucleus of fertilized FVB/N zygotes and implanted into pseudopregnant females. Six out of 114 mice obtained, which all appeared phenotypically normal, were germline transmitters, but only 2 founder lines expressed detectable levels of N1-Gal4VP16 mRNA in thymocytes (data not shown).

We further characterized these two N1-Gal4VP16 founders by crossing them with a UAS-LacZ transgenic mouse line carrying a LacZ reporter gene under the control of a promoter containing six Gal4 binding sites (Govindarajan *et al*., 2005). Consequently, in double-transgenic (DBL-Tg) mice, ligand-specific activation of the chimeric Notch1 receptor results in the release of the GAL4-VP16 protein, which translocates into the nucleus resulting in LacZ reporter activation (Fig. 1a).

Notch1 signaling is essential for the normal development of multiple organs during embryogenesis. At embryonic day (E) 13.5 we observe a widespread, but specific β-galactosidase staining in DBL-Tg embryos (Fig. 2a,c–k), but not in UAS-LacZ littermates (Fig. 2b). In the developing central nervous system (CNS), LacZ-activity was predominantly detected in the medulla oblongata, the pons (Fig. 2c) and in the spinal cord (Fig. 2d). It has been reported that segmentation of the somites depends on active Notch1 signaling (Conlon *et al*., 1995). Accordingly, N1-Gal4VP16/UAS-LacZ mice revealed β-galactosidase expression in the clefts between the growing somites (Fig. 2d). Proteolytic cleavage of the N1-Gal4VP16 transgene was also detected in the developing heart at E13.5 (Fig. 2e). Notch1 signaling was shown to be important for digit formation and to be expressed at the apical ectodermal ridge (AER) from E10.5 onwards (Francis *et al*., 2005). Concurrent with this report, N1-Gal4VP16 activity in the AER was observed at E10.5 (Fig. 2f), E12.5 (Fig. 2g), and E13.5 (Fig. 2h). Moreover, Notch1 activation is crucial for the formation of the vasculature during embryogenesis (Krebs *et al*., 2000). In agreement with these findings, we show that maturing blood vessels in double transgenic mice at E18.5 positively stain for β-galactosidase, presented by blood vessels at the surface of the brain (Fig. 2i) and in the dermis (Fig. 2j,k). Costaining with the endothelial cell marker CD31 and X-Gal confirms that N1-GALVP16 driven reporter activity was restricted to endothelial cells (Fig. 2k).

Analysis of X-Gal stained adult back skin and vibrissae established that N1-GalVp16 is continuously active in the sebaceous glands (SG) of hair follicles (HFs) and vibrissae (Fig. 3a–g). N1GalVp16 activity in the inner root sheet and the differentiating cells above the line of Auber (Au) was observed only during anagen phase of the hair cycle (Fig. 3a,e,f). In addition, during telogen and early anagen HFs exhibit LacZ-staining in the isthmus (Fig. 3c,d). Moreover, in both anagen and catagen

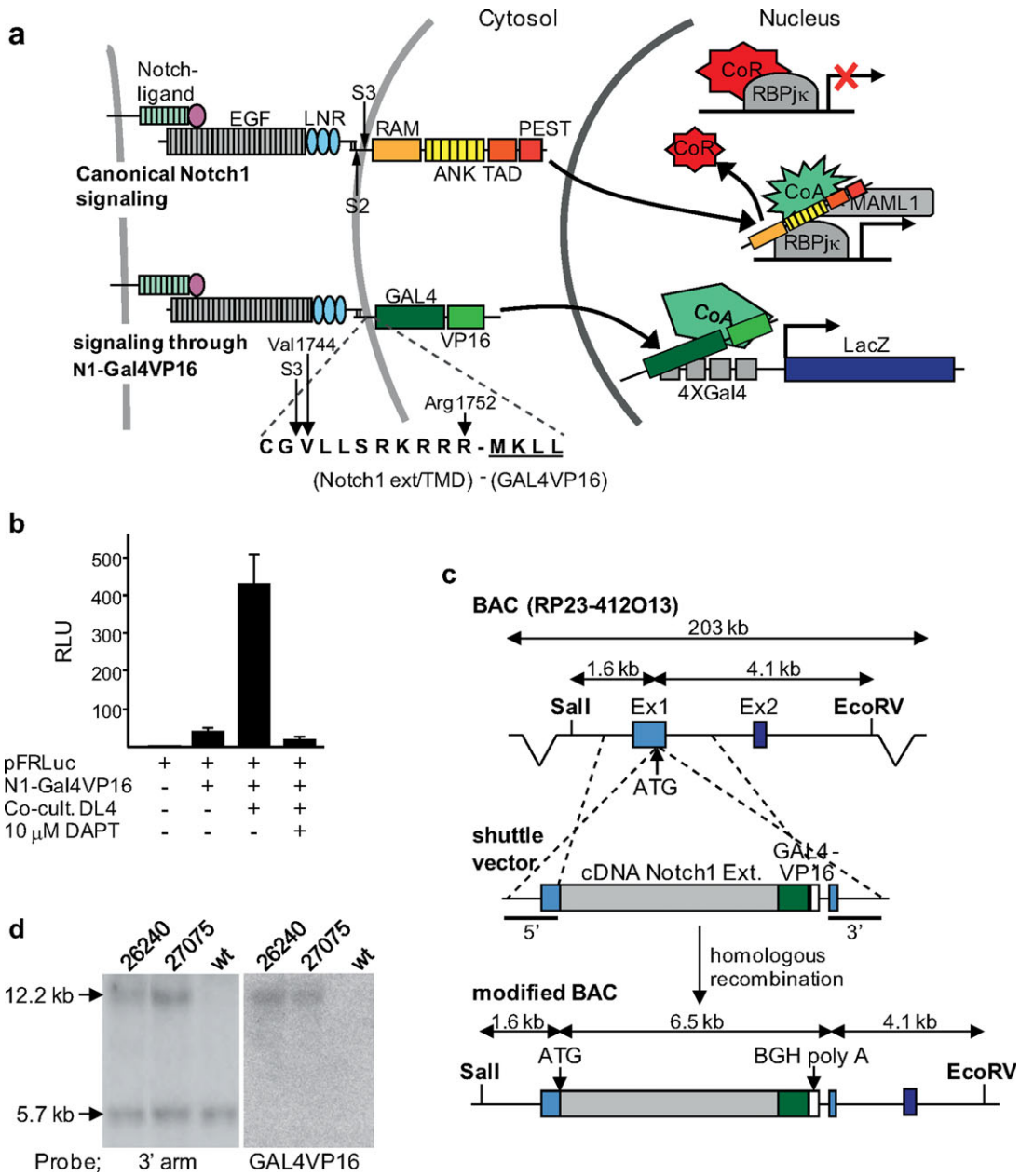

FIG. 1. Generation of the N1-Gal4VP16 mouse founder lines. (**a**) Outline of the protein structure and the signaling pathway of the endogenous Notch1 receptor (top) and the modified receptor, N1-Gal4VP16 (bottom). The Notch1 receptor is presented on the cell surface as a heterodimer. The engagement of the Notch1 extracellular domain with its ligand triggers two consecutive proteolytic cleavages, S2 and S3, which leads to the release of the Notch intracellular domain (NIC). In the nucleus, NIC forms a binary complex with RBPjκ, which recruits coactivators (CoA) to form the transcription-activating complex. In our model system, the NIC was replaced by the highly potent transcription factor Gal4-VP16. The shift from Notch1 to Gal4VP16 is at Arg1752, and consequently S2 and S3 are preserved in the fusion protein. Hence, interaction between an endogenous Notch ligand and the chimeric N1-Gal4VP16 receptor results in the proteolytic cleavage of the receptor followed by translocation of the Gal4VP16 protein into the nucleus, where it activates the expression of a Gal4-dependent *LacZ* reporter gene. EGF, epidermal growth factor-like repeats; LNR, Lin-Notch repeats; RAM, ram domain; ANK, ankyrin repeats; TAD, transactivation domain; PEST, PEST domain. (**b**) Functional assessment of the *N1-Gal4VP16* construct in vitro. Relative luciferase activity was detected in HeLa cells transiently transfected with a reporter plasmid under the control of five Gal4 binding sites (*pFRLuc*), along with *pBluescript* or a *N1-Gal4VP16* expression plasmid. Twelve hours after transfection, cells were cocultured for 24 h with HeLa cells expressing the Notch ligand Delta-like4 (DL4), with or without the γ-secretase inhibitor DAPT (10 μM), as indicated. Data shown is a representative of three transfection experiments normalized to the internal *TK-Renilla* control. Reporter activities obtained upon cotransfecting *pBluescript* and *pFRLuc* were normalized to one, and error bars indicate SD. (**c**) Illustration of the strategy to generate the modified BAC integrated with the N1-Gal4VP16 cassette into the ATG of the mouse *Notch1* gene. The shuttle vector contained a targeting construct of a 6.5 kb *N1-Gal4VP16* sequence flanked by a 1.1 kb 5′ and 1.2 kb 3′ arm of homology, respectively. The modified BAC, shown at the bottom, is a product of homologous recombination between the wt BAC and the shuttle vector. Transgenic mouse lines were established by injections of the modified BAC into the pronuclei of fertilized FVB/N oocytes. *Notch1* exon 1 and 2 are shown as light blue and blue squares, respectively, the *Notch*1 extracellular domain in light gray, *Gal4VP16* in green, and the BGH polyA tail in white. (**d**) Southern-blot analysis of N1-Gal4VP16 transgenic founder lines. Genomic DNA was digested SalI/EcoRV and hybridized with ^{32}P-labelled PCR-products corresponding to the 3′-homologous arm or Gal4VP16 as indicated. The blot shows the *N1-Gal4VP16* (12.2 kb) transgenic band for two N1-Gal4VP16 founder lines (26240 and 27075). The 5.7 kb band corresponds to the wt Notch1 alleles.

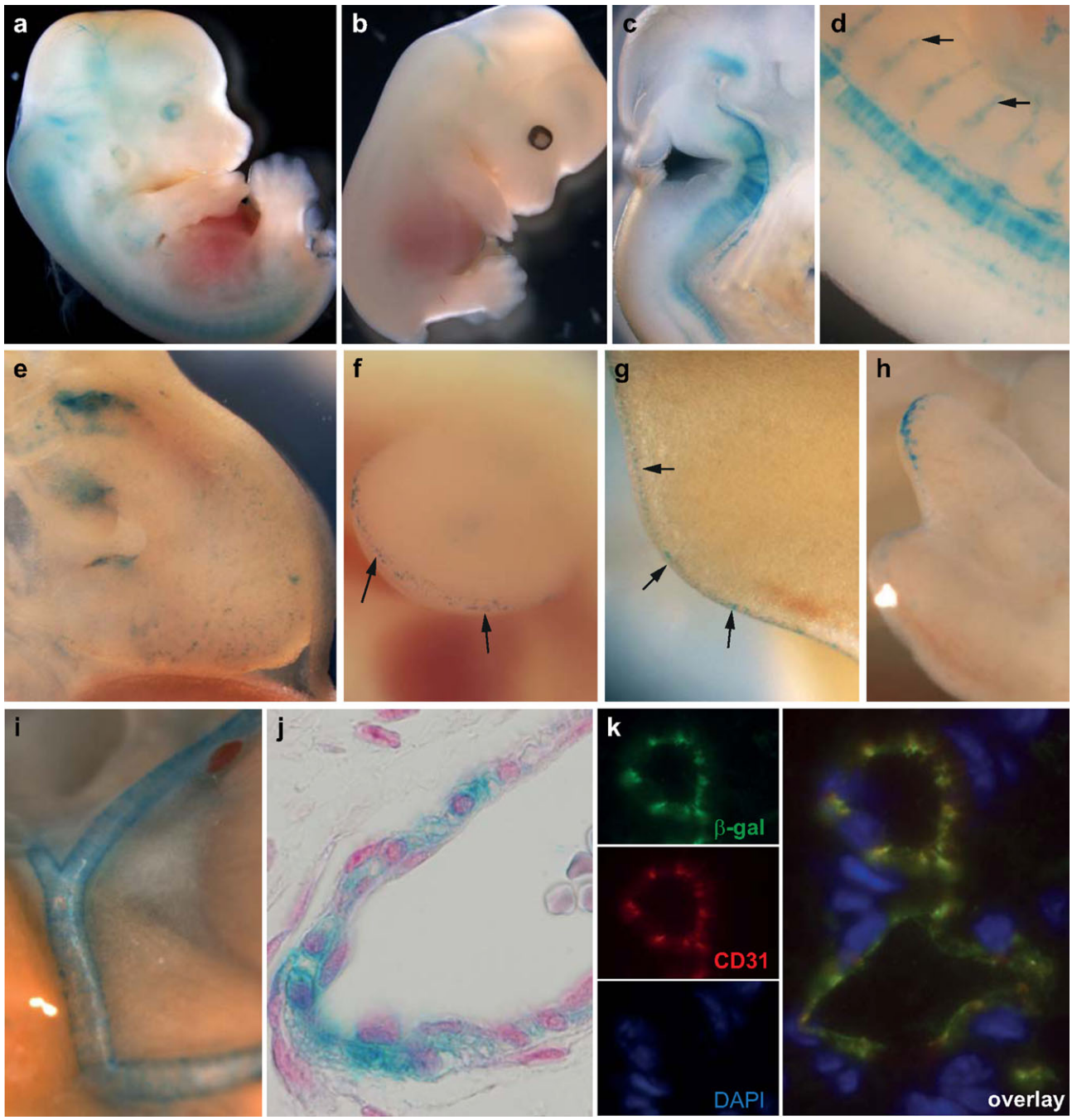

FIG. 2. Active Notch1 signaling visualized through N1-Gal4VP16 activity during embryonic development. (**a–k**) Whole mount β-galactosidase staining of transgenic embryos: (a) N1-Gal4VP16/UAS-LacZ and (b) UAS-LacZ embryos at E13.5. (c,d) Sections (500 μm) of a X-Gal stained E13.5 DBL-Tg embryo showing high N1-Gal4VP16 activity in (c) the medulla oblongata and (d) in the spinal cord and clefts between the forming somites (arrows). (e) N1-Gal4VP16 activity in the developing heart of an E13.5 N1-Gal4VP16/UAS-LacZ embryo. (f–h) A streak of LacZ staining (arrows) was apparent in the AER of (f) E10.5, (g) E12.5, and (h) E13.5 N1-Gal4VP16/UAS-LacZ embryos. (i) Ventral view of the brain from an E18.5 N1-Gal4VP16/UAS-LacZ mouse showing LacZ staining in cerebral arteries. (j) Notch1 signaling is active in the endothelium of the skin at E18.5 as demonstrated by (j) X-Gal staining and (k) antibodies directed against β-galactosidase and the endothelial cell marker CD31. Separate images of the respective fluorochrome channels are shown to the left of the merged image.

whiskers the differentiated cells, but not the basally located stem cells in the bulge region, stained positive for N1-GALVP16 driven β-galactosidase activity (Fig. 3f,g). The timing of hair morphogenesis and of the first hair cycle in the DBL-Tg mice was identical to control animals (data not shown) (Alonso and Fuchs, 2006;

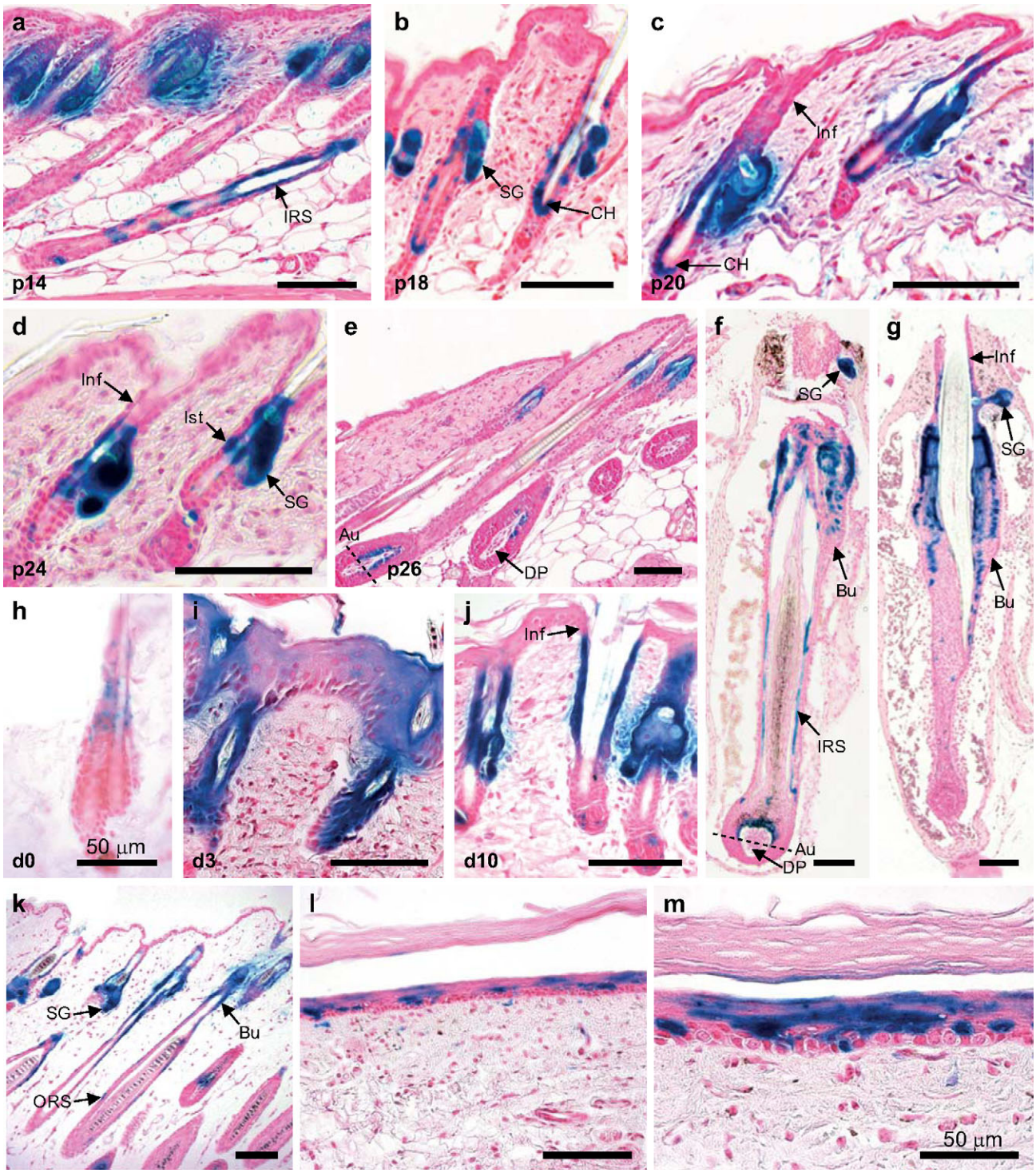

FIG. 3. N1-Gal4VP16 activity reflects active Notch1 signaling in the hair follicle. (**a–e**) Cross-sections of whole mount X-Gal stained backskin of N1-Gal4VP16 mice at (a) p14 (anagen), (b) p18 (catagen), (c) p20 (telogen), (d, e) p24 and p26 (first postnatal anagen). (f, g) Cross-section of whole mount X-Gal stained vibrissae in (f) anagen and (g) catagen phase. (**h–j**) X-Gal stained backskin 0, 3, and 10 days following dermabrasion. (**k–m**) Cross-section of X-Gal stained N1-Gal4VP16/UAS-LacZ skin from (k) the snout region and (l, m) the footpad. Nuclei are counterstained with nuclear fast red, and appear pink. Scale bars = 100 μm or as indicated. IRS, inner root sheath; SG, sebaceous gland; Bu, bulge; DP, dermal papilla; Ist, isthmus; Inf, infundibulum, CH, club hair, Au, line of Auber; ORS, outer root sheet.

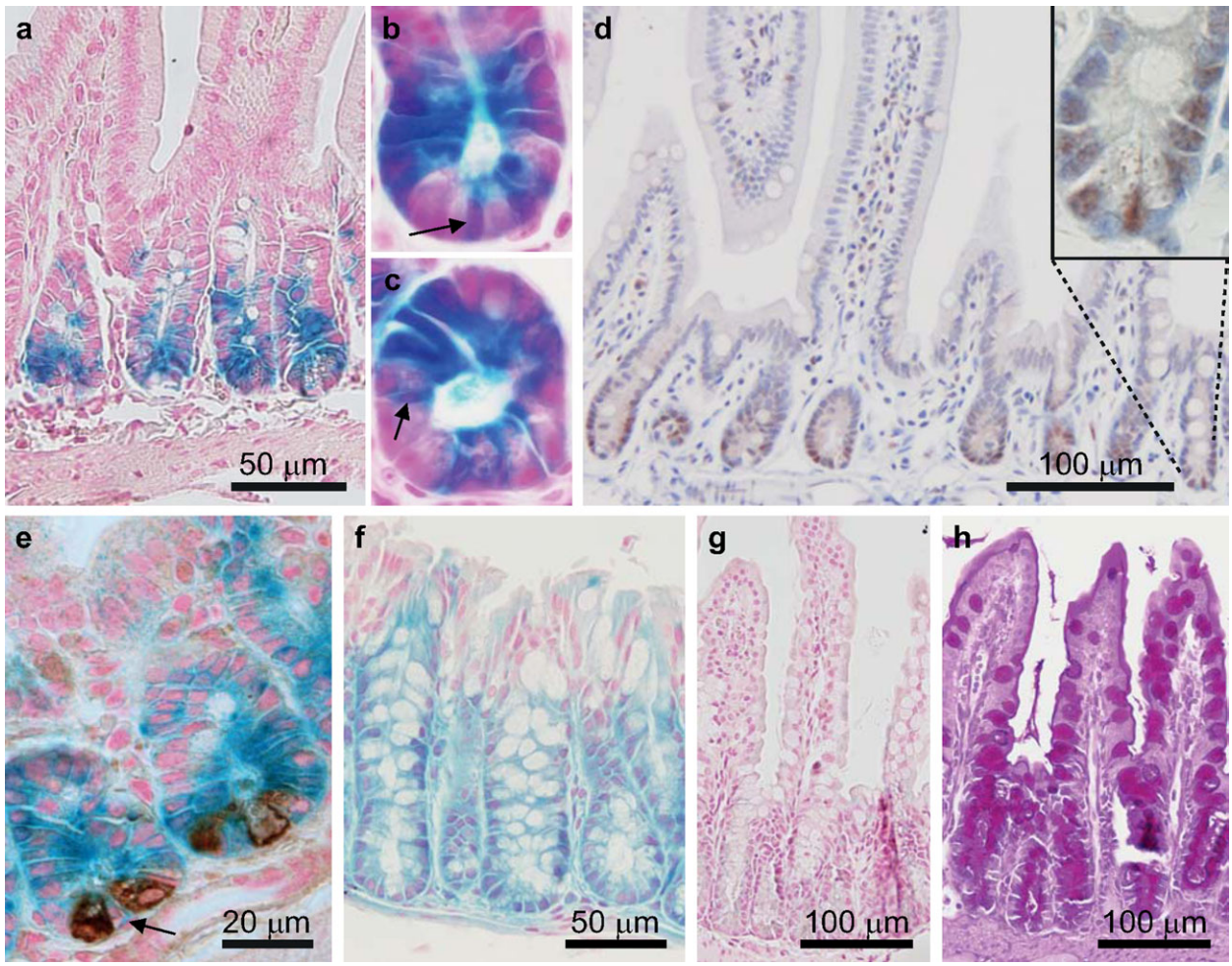

FIG. 4. N1-GalVP16 activity is restricted to the intestinal crypt. (**a–c**) Whole mount X-Gal stained duodenum from adult N1-Gal4VP16/UAS-LacZ mice. (a) 4 μm paraffin section and (b, c) 6 μm frozen sections showing β-galactosidase positive cells wedged between the Paneth cells (arrows) at the crypt base. (**d**) Immunohistological staining of wild type duodenum with the cleaved Notch1 (Val1744) antibody confirms that Notch1 activity is restricted to the intestinal crypt and is present in cells wedged between the Paneth cells (inset). (**e**) Lysozyme staining marking the Paneth cells in a cross-section of whole mount X-Gal stained N1-Gal4VP16/UAS-LacZ duodenum. (**f**) Whole mount X-Gal stained paraffin sections of N1-Gal4VP16/UAS-LacZ colon. (**g, h**) Whole mount X-Gal stained intestine from a DBZ-treated 21 day old N1-Gal4VP16/UAS-LacZ mouse. (h) Goblet cells stained by a Periodic Acid Schiff (PAS) staining.

Paus and Foitzik, 2004). Dermabrasion studies performed on DBL-Tg mice suggest that Notch1 signal-receiving cells contribute to the regeneration of HFs and epidermis (Fig. 3h–j). HFs from the snout area display β-galactosidase positive cells in the SG, outer root sheet, and the bulge (Fig. 3k). Units of N1-GalVP16 activity were also detected in the footpad (Fig. 3l), with sporadic staining in the basal layer (Fig. 3m).

X-Gal staining of intestinal segments from DBL-Tg animals indicates that Notch1 activity is restricted to the intestinal crypts in the duodenum (Fig. 4a), as well as in the jejunum and ileum (data not shown). Notch1 signaling has been proposed to be active in crypt progenitors and in $Lgr5^{+}$ stem cells at the bottom of the intestinal crypt (Pellegrinet *et al*., 2011). Indeed, cells at the crypt base of the DBL-Tg mice revealed β-galactosidase staining in crypt progenitors and in intestinal stem cells wedged between the Paneth cells (Fig. 4b,c). This notion was further confirmed upon costaining with the Paneth cell marker lysozyme (Fig. 4e). Staining of wild type duodenum for cleaved Notch1 using the Val1744 antibody established that the N1-GalVP16 activity is indeed representative for Notch1 activation in the intestine (Fig. 4d). In addition, LacZ-activity was observed in the colon at the crypt base as well as in the proliferative compartment (Fig. 4f). To further confirm the in vivo γ-secretase-dependent activation of the N1-GALVP16 fusion protein, DBL-Tg mice were treated with the γ-secretase inhibitor dibenzazepine (DBZ). The absence of LacZ-positive cells accompanied with goblet cell

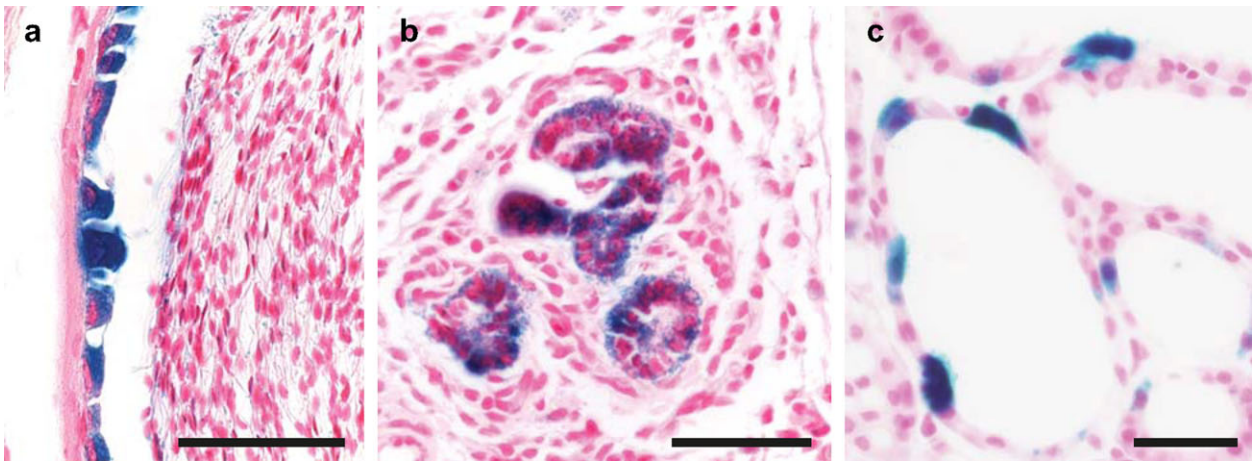

FIG. 5. Cells within reproductive organs and mammary glands display N1-Gal4VP16 activity. (**a, b**) Whole mount X-Gal staining of adult N1-Gal4VP16/UAS-LacZ (a) epididymis and (b) uterus reveal β-galactosidase positive cells in the (a) pseudostratified columnar epithelial cells of the epididymis wall and (b) the endometrial uterine glands. (**c**) X-Gal staining of a frozen section of a mammary gland from a N1-Gal4VP16/UAS-LacZ-positive lactating female show interspersed N1-Gal4Vp16 activation in the luminal epithelial cells of the lobular aveoli. Scale bars = 50 μm.

metaplasia in the small intestine indicated a complete block of endogenous Notch signaling as well as N1-Gal4VP16 activity (Fig. 4g,h), which is in agreement with previous reports (Pellegrinet *et al*., 2011).

Reproductive organs revealed specific LacZ-staining in the pseudostratified columnar epithelial cells of the epididymis wall (Fig. 5a) and in the uterine glands (Fig. 5b). Notch1-activity was not observed in the testis or mature spermatozoa (data not shown). In the mammary gland from a lactating female, scattered luminal epithelial cells were LacZ-positive (Fig. 5c), while no N1-Gal4VP16-activity was observed in the mammary glands from virgin females (data not shown).

In the adult brain, Notch1 reporter activity was most distinct in the lateral ventricles (LV), but also present in astrocytes (Fig. 6a,c). No LacZ-positive cells were detected in the brain of UAS-LacZ littermate control animals (Fig. 6b). Staining of wild type brain with the anti-Val1744 antibody confirms that endogenous Notch1 activity is mirrored by the pattern of reporter activity (Fig. 6d). This is in agreement with data from Carlén *et al*., stating that ependymal cells lining the LV wall receive active Notch1 signals (Carlen *et al*., 2009).

Taken together, the N1-Gal4VP16 activity observed in our BAC-transgenic reporter mice correlates well with the expected profile of active Notch1 signaling based on established knowledge and antibody staining assays. Thus, we conclude that the activation of the N1-Gal4VP16 is consistent with the activity of the endogenous Notch1 receptor. Moreover, this reporter mouse is a powerful tool, which enables the visualization of active Notch1 signaling in embryonic and post-natal development in vivo.

MATERIAL AND METHODS

Mice

The *N1-Gal4VP16* targeting vector was generated by replacing the intracellular domain of the Notch1 receptor with a cDNA fragment encoding for *Gal4VP16*. Furthermore, a 1.1 kb and a 1.2 kb fragment immediately upstream and downstream of the endogenous *Notch1* ATG were amplified by PCR (68°C, 30 cycles) using primer pairs #1 (5′-TTACGAACGCGTGGCGCGCCAACTCTGCACTTTCCCAGGCCACCTAAG-3′) and #2 (5′-TACTCCAAGCTTGCCTGCTCGCCAGCTGCCCGCAGCC-3′), #3 (5′-TTACGAACCGGTCCACGGCTCCTGACGCCCTTGCTCT-3′), and #4 (5′-TACTCCTTAATTAAGTTCAAACACAAGATACGAGGGGACCG-3′) and a BAC clone (RP23-412O13, CHORI BACPAC Resources Center, Oakland, CA) encoding the complete mouse Notch1 gene locus as a template. The purified PCR fragments were cloned upstream of the *N1-Gal4VP16* ATG, and downstream of the cDNA3.1 bovine growth hormone (BGH) polyA tail. The whole recombination cassette, *N1-Gal4VP16* including the homologous arms, was transferred to the shuttle vector pLD53.SC-AB (Gong *et al*., 2002; Metcalf *et al*., 1996) (kindly received from Dr. Gerard Eberl) and inserted into the site of the *Notch1* ATG in the wild-type BAC, via a two-step homologous recombination as previously described (Gong *et al*., 2002; Sparwasser *et al*., 2004). Briefly, the shuttle vector carrying the *N1-Gal4VP16* recombination cassette was electroporated into the BAC-containing bacteria (DH10B *RecA*$^-$ cells), and selected on Luria broth (LB) agar plates containing chloramphenicol (12.5 μg/ml) and ampicillin (50 μg/ml). Successful integration of the shuttle vector into the BAC was confirmed by PCR

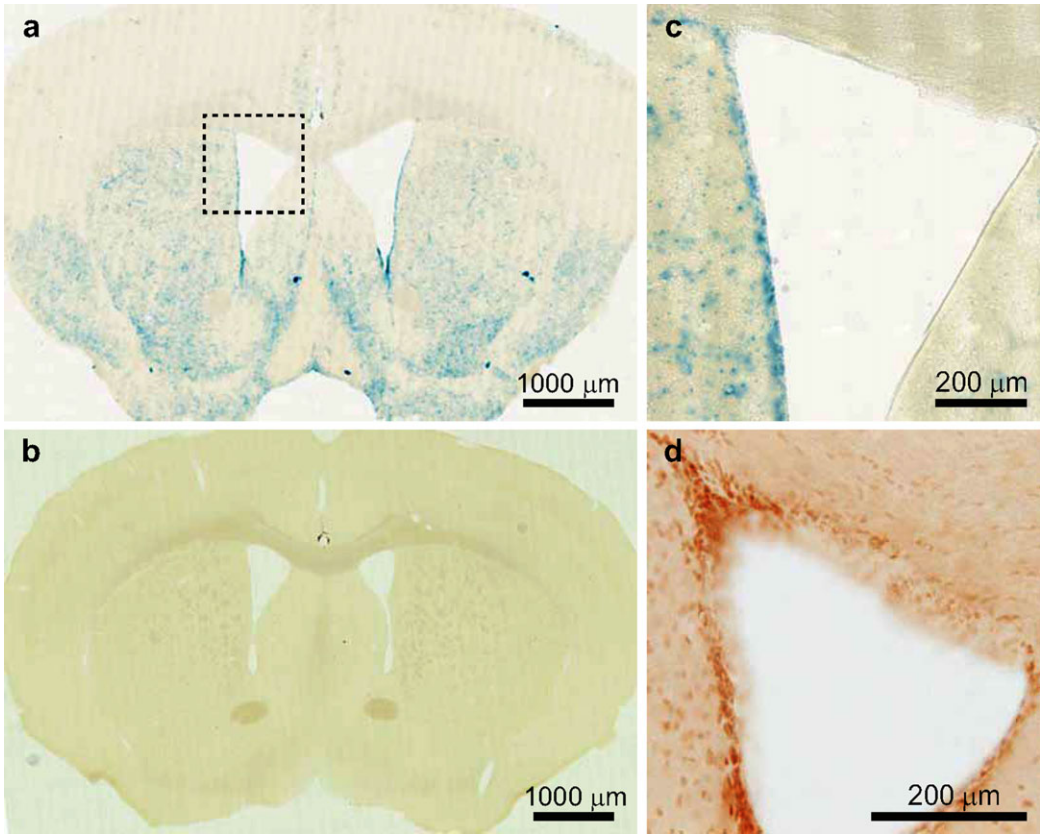

FIG. 6. N1-Gal4VP16 activity mirrors active Notch1 signaling in the brain. (**a–c**) X-Gal staining of 35 μm thick free floating brain sections from (a, c) a double transgenic mouse, and (b) a UAS-LacZ positive littermate control. (c) Magnification of the left lateral ventricle (LV), stippled box in (a). (**d**) Immunohistochemistry staining of 35 μm wild type brain free floating sections with cleaved Notch1 (Val1744) antibody confirms high Notch1 activity in the LV.

using the following primer pairs: #5 (5′-AAAGGGATAAGGAAGGCATCTTGGACGC-3′) and #6 (5′-AGTAGCTTGTATTCTATAGTGTCACC-3′), or #7 (5′-TAGGGTGATGGTTCACGTAGTGCG-3′) and #8 (5′-ACACAGCCAAAGTGGGAGGGGATTAAGG-3′).

Colonies positive for double integration were selected again on LB-agar plates containing chloramphenicol (12.5 μg/ml) and sucrose (5%). Resolved and modified BAC clones were identified by PCR with primer pairs listed above, and by Southern blot analysis using a ^{32}P-labeled probe specific for the 3′ homologous arm (for details see below). The modified BAC DNA was purified and injected into pronuclei of fertilized FVB/N zygotes. Offspring was typed for the presence of the *N1-Gal4VP16* transgene using the following primers pairs: #9 (5′-CTAGGTGCTCTTGCGTCACTTGGC-3′) and #10 (5′-CTCCACTGAAGCCAATCTATCTGTG-3′).

Founder lines typed positive for the transgene N1-Gal4VP16 by PCR were also verified by Southern blot analysis (see details below). Heterozygous *N1-Gal4VP16* mice were subsequently crossed with the *UAS-lacZ* transgenic reporter mice, kindly provided by Dr. P. Overbeek, Houston (Govindarajan *et al.*, 2005). The *UAS-lacZ* mice were genotyped with primers specific for the *lacZ* gene: #11 (5′-CCCATTACGGTCAATCCGCCG-3′) and #12 (5′-GCCTCCAGTACAGCGCGGCTG-3′).

Details for individual PCR reactions will be provided upon request. This transgenic Notch1 signaling specific reporter mouse line will be available to the research community upon acceptance of the manuscript.

The γ-secretase inhibitor DBZ (25 μM/kg body weight in dimethyl sulfoxide (DMSO); Calbiochem, San Diego, CA) was injected intraperitoneally for four consecutive days. Mice were analyzed 24 h after the last injection.

Ethics Statement

All animal work was conducted according to Swiss national guidelines and under EPFL animal care regulations. They were housed in individual cages at (23 ± 1)°C with a 12 h light/dark cycle. All animals were supplied with food and water ad libitum. This study has been reviewed and approved by the Service Vétérinaire Cantonal of Etat de Vaud.

Southern Blot Hybridization

Southern blot hybridizations were performed following standard procedures. Briefly, 20 μg of BAC or genomic tail DNA were digested with SalI/EcoRV restriction enzymes and resolved in an 0.8% agarose gel. Digested DNA was transferred onto a Hybond-N+ nylon membrane (GE Healthcare Life Sciences, Buckinghamshire, UK) and hybridized overnight at 65°C with either a ^{32}P-labelled PCR product corresponding to the 3′-homologous arm or a ^{32}P-labelled 700 bp *Gal4VP16* fragment amplified using the following primers: #13 (5′-GCGCATGAAGCTACTGTCTTCTA TCG-3′) and #14 (5′-GCTACCCACCGTACTCGTCAA TTCC-3′).

Positive labeled *N1-Gal4VP16* transgenic samples were visualized using a Phosphorimager (FLA3000; Fujifilm).

Tissue Culture Conditions, Transfections, and Luciferase assays

HeLa cells were cultured at 37°C and 5% CO_2 in Dulbecco's Modified Eagle's Medium (DMEM) (high glucose, GlutaMAX™-I) medium supplemented with 10% fetal calf sreum (FCS) and 0.1 mg/ml Penicillin/Streptomycin (all purchased from Gibco®, Invitrogen Corporation, Paisley, UK). HeLa cells seeded into a 12-well tissue culture plate were transiently transfected with 2 μg of a *DL4* expression plasmid, or 1 μg *pFR-Luc* (Stratagene, Offenbach, Germany) and 50 ng of *prL-TK* (Promega Corporation, Madison, WI) reporter plasmids, along with 1 μg *pBluescript* (Stratagene, Offenbach, Germany) and the *N1-Gal4VP16* expression plasmid using the transfection reagent JetPEI™ (PolyPlus Transfection, Illkirch, France) according to the manufacturer's recommendations. In order to induce N1-GAL4VP16 driven activation of the reporter gene, N1-GAL4VP16 expressing cells were cocultured with DL4 expressing HeLa cells in a 1:1 ratio in the presence or absence of 10 μM DAPT (Merck & Co., New Jersey, USA). Twenty-four hour post-coculture, cells were lysed using 250 μl of passive lysis buffer and the luciferase assay was performed with a Dual-Luciferase™ Reporter Assay System (Promega Corporation, Madison, WI) using 20 μl of the total protein extract. All samples were analyzed in triplicates.

X-Gal Staining

Whole mount embryos (10.5–14.5 dpc) as well as dissected whole mount organs (18.5 dpc to adult mice) were fixed at 4°C in LacZ fixative (0.2% glutaraldehyde, 5 mM EGTA (pH 7.3) and 4 mM $MgCl_2$ in 0.1M sodium phosphate buffer (pH 7.3)), washed three times in detergent wash (2 mM $MgCl_2$, 0.01% desoxycholate, and 0.02% NP40 in 0.1 M sodium phosphate buffer (pH 7.3)), and stained for β-galactosidase activity for 2–24 h at 37°C in detergent wash supplemented with 0.66 mg/ml X-Gal, 3.33 mM $K_3Fe(CN)_6$, 3.33 mM $K_4Fe(CN)_6$, and 20 mM Tris–HCl (pH 7.3). Subsequently, the embryos and organs were rinsed in 1× PBS and postfixed for 1–3 h in 4% paraformaldehyde (PFA). Embryos were photographed as whole mount, or embedded in 5% agarose in 1× phosphate buffered saline (PBS) and sectioned at 500 μm using a vibratome. For histology, whole mount stained tissues were dehydrated, paraffin embedded, sectioned at 4 μm, and counterstained with Nuclear Fast Red according to standard procedures. X-Gal stained whiskers and intestine were embedded in optimal cutting temrature (OCT) tissue matrix and processed as described above. β-Galactosidase activity in the adult brain of transgenic mice was visualized after transcardial perfusion using 4% PFA. Brains were postfixed for 1 h at 4°C in 4% PFA, cryoprotected in 30% sucrose over night, embedded in OCT, cut in 35 μm free floating coronal sections, and stained as described above.

Immunohistochemistry

Immunofluorescent costaining for CD31 and β-galactosidase were done on sections (6 μm) of fresh frozen skin. The sections were fixed in methanol, blocked in 1% bovine serum albumine (BSA), and stained at 4°C overnight with the following primary antibodies; monoclonal rat anti-mouse CD31 (1:100 dilution; BD Pharmingen, BD biosciences, San Jose, CA) and polyclonal goat anti-β-galactosidase (1:150 dilution; Biogenesis, AbD Serotac, Oxon, UK). Alexa Fluor 568 goat anti-rat IgG (dilution 1/1000; Molecular Probes, Life Technologies Corporation), and Alexa Fluor 488 donkey anti-goat IgG (dilution 1/800; Molecular Probes, Life Technologies, Carlsbad, CA) were used as secondary antibodies, and nuclei counterstained with DAPI. Lysozyme staining was performed on paraffin sections of whole mount X-Gal stained intestinal samples. Sections were dewaxed, rehydrated, pretreated with peroxidase (5 min, 3% H_2O_2), antigen retrieved (20 min at 95°C in 10 mM sodium citrate buffer pH 6.0), and stained with a rabbit anti-lysozyme antibody (1:500 dilution overnight at 4°C; DAKO, Glostrup, Denmark). HRP-labeled anti-rabbit antibody was used for second stage staining and the chromogen-substrate was detected with DAB revelation (Sigma, St. Louis, MO). Sections from whole mount X-Gal stained intestine DBZ-treated mice were stained using the Periodic acid-Schiff (PAS) technique and counterstained with Mayer's Hematoxylin. Cleaved Notch1 was detected on sections of 4% PFA-fixed paraffin embedded wild type intestine. Antigen retrieval was performed in DIVA decloaker buffer (Biocare medical, Concord, CA) and sections were incubated with a primary rabbit polyclonal antibody raised against cleaved Notch1 Val1744 (1:300 dilution overnight at 4°C; Abcam, Cambridge, UK). Sections were then incubated with horseradish peroxidase (HRP) labeled polymers

conjugated to goat anti-rabbit immunoglobulins (EnVision+ System, DAKO, Glostrup, Denmark) and the staining was visualized with DAB revelation (Sigma, St. Louis, MO). Cleaved Notch1 in the brain was revealed on 35 μm free floating sections of wild type mice perfused with 4% PFA. Sections were treated with 1N HCl for 30 min at 65°C, quenched for 15 min at RT [3% H_2O_2 and 10% methanol in 0.1 M potassium phosphate buffered saline (KPBS)] and incubated for 1 h in blocking solution (5% normal serum and 0.25% Triton-X in KPBS). Subsequently, sections were stained with a primary antibody directed against cleaved Notch1 Val1744 (1:200 dilution in blocking solution overnight at RT; Abcam, Cambridge, UK). A biotinylated goat anti-rabbit IgG secondary antibody (Vector Laboratories, Burlingame, CA) was then applied for 1 h at RT. Antibody binding was visualized using the Vectastain ABC kit (Vector Laboratories, Burlingame, CA) and DAB-revelation.

ACKNOWLEDGMENTS

Authors thank Dr. Gerard Eberl for providing the BAC specific shuttle vector, Dr. Paul A. Overbeek for the UAS-LacZ mice, Louis Mercier for technical help, Dr. Johan Jakobsson, and Malin Åkerblom for the interpretation of the LacZ-staining in the brain, and Dr. Craig Nowell and Dr. Ute Koch for critical reading of the manuscript. The authors have no conflict of interest.

LITERATURE CITED

Alonso L, Fuchs E. 2006. The hair cycle. J Cell Sci 119:391–393.

Artavanis-Tsakonas S, Muskavitch MA. 2010. Notch: The past, the present, and the future. Curr Top Dev Biol 92:1–29.

Basak O, Taylor V. 2007. Identification of self-replicating multipotent progenitors in the embryonic nervous system by high Notch activity and Hes5 expression. Eur J Neurosci 25:1006–1022.

Brou C, Logeat F, Gupta N, Bessia C, LeBail O, Doedens JR, Cumano A, Roux P, Black RA, Israel A. 2000. A novel proteolytic cleavage involved in Notch signaling: The role of the disintegrin-metalloprotease TACE. Mol Cell 5:207–216.

Carlen M, Meletis K, Goritz C, Darsalia V, Evergren E, Tanigaki K, Amendola M, Barnabe-Heider F, Yeung MS, Naldini L, Honjo T, Kokaia Z, Shupliakov O, Cassidy RM, Lindvall O, Frisen J. 2009. Forebrain ependymal cells are Notch-dependent and generate neuroblasts and astrocytes after stroke. Nat Neurosci 12:259–267.

Conlon RA, Reaume AG, Rossant J. 1995. Notch1 is required for the coordinate segmentation of somites. Development 121:1533–1545.

De Strooper B, Annaert W, Cupers P, Saftig P, Craessaerts K, Mumm JS, Schroeter EH, Schrijvers V, Wolfe MS, Ray WJ, Goate A, Kopan R. 1999. A presenilin-1-dependent gamma-secretase-like protease mediates release of Notch intracellular domain. Nature 398:518–522.

Duncan AW, Rattis FM, DiMascio LN, Congdon KL, Pazianos G, Zhao C, Yoon K, Cook JM, Willert K, Gaiano N, Reya T. 2005. Integration of Notch and Wnt signaling in hematopoietic stem cell maintenance. Nat Immunol 6:314–322.

Fortini ME, Artavanis-Tsakonas S. 1994. The suppressor of hairless protein participates in notch receptor signaling. Cell 79:273–282.

Francis JC, Radtke F, Logan MP. 2005. Notch1 signals through Jagged2 to regulate apoptosis in the apical ectodermal ridge of the developing limb bud. Dev Dyn 234:1006–1015.

Fre S, Hannezo E, Sale S, Huyghe M, Lafkas D, Kissel H, Louvi A, Greve J, Louvard D, Artavanis-Tsakonas S. 2011. Notch lineages and activity in intestinal stem cells determined by a new set of knock-in mice. PLoS One 6:e25785.

Gong S, Yang XW, Li C, Heintz N. 2002. Highly efficient modification of bacterial artificial chromosomes (BACs) using novel shuttle vectors containing the R6Kgamma origin of replication. Genome Res 12:1992–1998.

Govindarajan V, Harrison WR, Xiao N, Liang D, Overbeek PA. 2005. Intracorneal positioning of the lens in Pax6-GAL4/VP16 transgenic mice. Mol Vis 11:876–886.

Imayoshi I, Sakamoto M, Yamaguchi M, Mori K, Kageyama R. 2010. Essential roles of Notch signaling in maintenance of neural stem cells in developing and adult brains. J Neurosci 30:3489–3498.

Jarriault S, Brou C, Logeat F, Schroeter EH, Kopan R, Israel A. 1995. Signalling downstream of activated mammalian Notch. Nature 377:355–358.

Krebs LT, Xue Y, Norton CR, Shutter JR, Maguire M, Sundberg JP, Gallahan D, Closson V, Kitajewski J, Callahan R, Smith GH, Stark KL, Gridley T. 2000. Notch signaling is essential for vascular morphogenesis in mice. Genes Dev 14:1343–1352.

Kurooka H, Honjo T. 2000. Functional interaction between the mouse notch1 intracellular region and histone acetyltransferases PCAF and GCN5. J Biol Chem 275:17211–17220.

Metcalf WW, Jiang W, Daniels LL, Kim SK, Haldimann A, Wanner BL. 1996. Conditionally replicative and conjugative plasmids carrying lacZ alpha for cloning, mutagenesis, and allele replacement in bacteria. Plasmid 35:1–13.

Mumm JS, Schroeter EH, Saxena MT, Griesemer A, Tian X, Pan DJ, Ray WJ, Kopan R. 2000. A ligand-induced extracellular cleavage regulates gamma-secretase-like proteolytic activation of Notch1. Mol Cell 5:197–206.

Ohtsuka T, Imayoshi I, Shimojo H, Nishi E, Kageyama R, McConnell SK. 2006. Visualization of embryonic neural stem cells using Hes promoters in transgenic mice. Mol Cell Neurosci 31:109–122.

Oswald F, Tauber B, Dobner T, Bourteele S, Kostezka U, Adler G, Liptay S, Schmid RM. 2001. p300 acts as a transcriptional coactivator for mammalian Notch-1. Mol Cell Biol 21:7761–7774.

Paus R, Foitzik K. 2004. In search of the "hair cycle clock": A guided tour. Differentiation 72: 489–511.

Pellegrinet L, Rodilla V, Liu Z, Chen S, Koch U, Espinosa L, Kaestner KH, Kopan R, Lewis J, Radtke F. 2011. Dll1- and dll4-mediated notch signaling are required for homeostasis of intestinal stem cells. Gastroenterology 140:1230–1240.e1231–1237.

Schroeter EH, Kisslinger JA, Kopan R. 1998. Notch-1 signalling requires ligand-induced proteolytic release of intracellular domain. Nature 393:382–386.

Souilhol C, Cormier S, Monet M, Vandormael-Pournin S, Joutel A, Babinet C, Cohen-Tannoudji M. 2006. Nas transgenic mouse line allows visualization of Notch pathway activity in vivo. Genesis 44: 277–286.

Sparwasser T, Gong S, Li JY, Eberl G. 2004. General method for the modification of different BAC types and the rapid generation of BAC transgenic mice. Genesis 38:39–50.

Struhl G, Adachi A. 1998. Nuclear access and action of notch in vivo. Cell 93:649–660.

Wallberg AE, Pedersen K, Lendahl U, Roeder RG. 2002. p300 and PCAF act cooperatively to mediate transcriptional activation from chromatin templates by notch intracellular domains in vitro. Mol Cell Biol 22:7812–7819.

Vooijs M, Ong CT, Hadland B, Huppert S, Liu Z, Korving J, van den Born M, Stappenbeck T, Wu Y, Clevers H, Kopan R. 2007. Mapping the consequence of Notch1 proteolysis in vivo with NIP-CRE. Development 134:535–544.

Wu L, Aster JC, Blacklow SC, Lake R, Artavanis-Tsakonas S, Griffin JD. 2000. MAML1, a human homologue of Drosophila mastermind, is a transcriptional coactivator for NOTCH receptors. Nat Genet 26:484–489.